

# xLSTM-SENet: xLSTM for Single-Channel Speech Enhancement

Nikolai Lund Kühne<sup>1</sup>, Jan Østergaard<sup>1</sup>, Jesper Jensen<sup>1,2</sup>, Zheng-Hua Tan<sup>1</sup>

<sup>1</sup>Department of Electronic Systems, Aalborg University, Denmark

<sup>2</sup>Oticon A/S, Copenhagen, Denmark

{nlk, jo, jje, zt}@es.aau.dk

## Abstract

While attention-based architectures, such as Conformers, excel in speech enhancement, they face challenges such as scalability with respect to input sequence length. In contrast, the recently proposed Extended Long Short-Term Memory (xLSTM) architecture offers linear scalability. However, xLSTM-based models remain unexplored for speech enhancement. This paper introduces xLSTM-SENet, the first xLSTM-based single-channel speech enhancement system. A direct comparative analysis reveals that xLSTM—and notably, even LSTM—can match or outperform state-of-the-art Mamba- and Conformer-based systems across various model sizes in speech enhancement on the VoiceBank+Demand dataset. Through ablation studies, we identify key architectural design choices such as exponential gating and bidirectionality contributing to its effectiveness. Our best xLSTM-based model, xLSTM-SENet2, outperforms state-of-the-art Mamba- and Conformer-based systems of similar complexity on the Voicebank+DEMAND dataset.

**Index Terms:** xLSTM, speech enhancement, LSTM, Mamba

## 1. Introduction

Real-world speech signals are often disrupted by noise, which degrades performance in hearing assistive devices [1], automatic speech recognition systems [2], and for speaker verification [3]. The process of removing background noise and enhancing the quality and intelligibility of the desired speech signal is known as speech enhancement (SE). Given the wide range of applications, SE has garnered significant research interest.

Single-channel SE methods leveraging deep learning [1] encompass a selection of architectures, such as recurrent Long Short-Term Memory (LSTM) networks [4], convolutional neural networks (CNNs) [5, 6], generative adversarial networks (GANs) [7–10], and diffusion models [11–13]. Recently, Conformer-based models have demonstrated impressive SE performance, achieving state-of-the-art results [10, 14] on the VoiceBank+Demand dataset [15, 16]. However, models based on scaled dot-product attention, such as Transformers and Conformers, face challenges with scalability with respect to input sequence length [17], and they require a lot of data to train [18].

To address the inherent limitations of attention-based models, Mamba [19], a sequence model integrating the strengths of CNNs, RNNs, and state space models, has recently emerged. Mamba has demonstrated competitive or superior performance relative to Transformers across various tasks, including audio classification [20] and SE [21].

On the other hand, recurrent neural networks (RNNs), particularly LSTMs [22], also offer several advantages over attention-based models, including: (i) linear scalability instead of quadratic, in terms of computational complexity with respect

to the input sequence length, and (ii) reduced runtime memory requirements, as they do not require storage of the full key-value (KV) cache. In contrast, attention-based models such as Transformers and Conformers necessitate significant memory overhead for KV storage. Despite these advantages, LSTMs suffer from critical drawbacks: (i) inability to revise storage decisions, (ii) reliance on scalar cell states, constraining storage capacity, and (iii) memory mixing preventing parallelizability [23]. Consequently, LSTMs have been less utilized in recent deep learning-based SE systems, with only a few exceptions [4, 24].

Recently, the Extended Long Short-Term Memory architecture (xLSTM) [23] was proposed to overcome the limitations of LSTMs. By incorporating exponential gating, matrix memory, and improved normalization and stabilization mechanisms while eliminating traditional memory mixing, xLSTM introduces two new fundamental building blocks: sLSTM and mLSTM. The xLSTM architecture has shown competitive performance across tasks such as natural language processing [23], computer vision [25], and audio classification [26]. However, while xLSTM adds increased memory via matrix memory and an improved ability to revise storage decisions via exponential gating, the potential advantages of these additions over LSTM have yet to be assessed for SE.

In this work, we propose an xLSTM-based SE system (xLSTM-SENet), which is the first single-channel SE system utilizing xLSTM. The system architecture is illustrated in Figure 1. Systematic comparisons of our proposed xLSTM-SENet with Mamba-, and Conformer-based counterparts across various model sizes, show that xLSTM-SENet matches the performance of state-of-the-art Mamba- and Conformer-based systems on the VoiceBank+Demand dataset [15, 16]. Intriguingly, upon an in depth investigation, we find that LSTMs can match or even outperform xLSTM, Mamba, and Conformers on the VoiceBank+Demand dataset. Additionally, we perform detailed ablation studies to explore the importance of multiple architectural design choices, quantifying their impact on overall performance. Finally, our best configured xLSTM-based model, xLSTM-SENet2, outperforms state-of-the-art Mamba- and Conformer-based systems of similar complexity on the Voicebank+DEMAND dataset. Code is publicly available.<sup>1</sup>

## 2. Method

### 2.1. Extended long short-term memory

As mentioned, xLSTM [23] introduces two novel building blocks: sLSTM and mLSTM, to address the limitations of the original LSTM [22]. Following Vision-LSTM [25] and Audio xLSTM [26], we employ mLSTM as the main building block

<sup>1</sup><https://github.com/NikolaiKyhne/xLSTM-SENet>

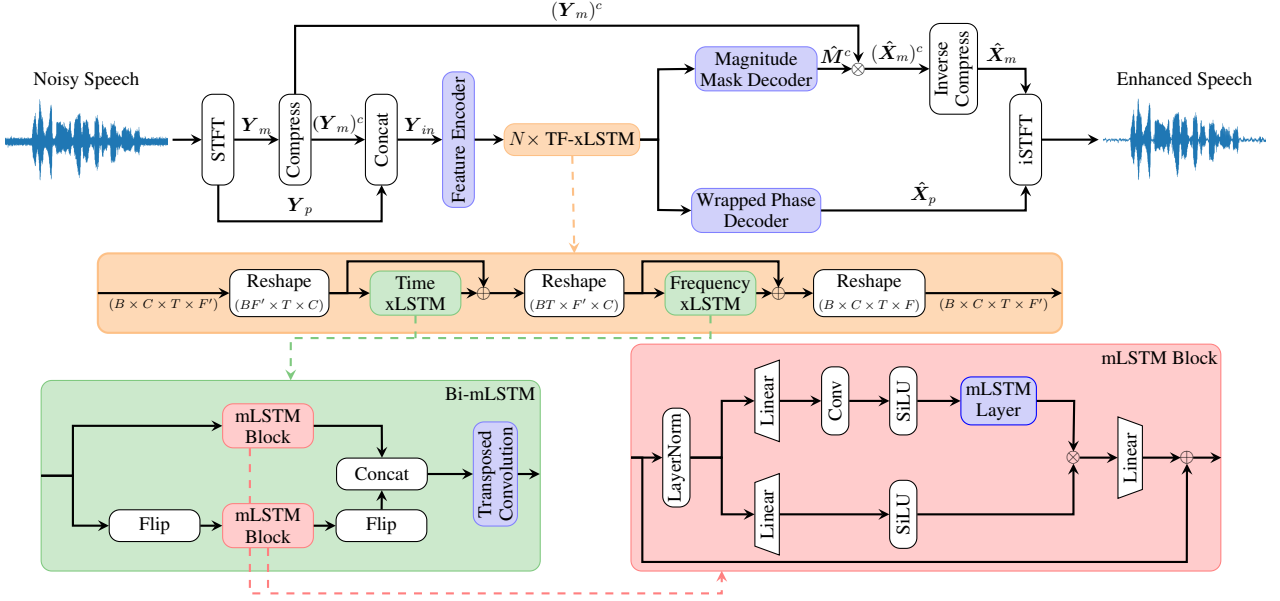


Figure 1: Overall structure of our proposed xLSTM-SENet with parallel magnitude and phase spectra denoising.

in our SE system. Unlike the sigmoid gating used in traditional LSTMs, mLSTM adopts exponential gating for the input and forget gates, enabling it to better revise storage decisions. Additionally, the scalar memory cell  $c \in \mathbb{R}$  is replaced with a matrix memory cell  $C \in \mathbb{R}^{d \times d}$  to increase storage capacity. Each mLSTM block projects the  $D$ -dimensional input by an expansion factor  $E_f \in \mathbb{N}$  to  $d = E_f D$  before projecting it back to  $D$ -dimensions after being processed by an mLSTM layer. The forward pass of mLSTM is given by [23]:

$$C_t = f_t C_{t-1} + i_t v_t k_t^\top, \quad (1)$$

$$n_t = f_t n_{t-1} + i_t k_t, \quad (2)$$

$$h_t = o_t \odot \left( C_t q_t / \max \{ |n_t^\top q_t|, 1 \} \right), \quad (3)$$

$$q_t = W_q x_t + b_q, \quad (4)$$

$$k_t = \frac{1}{\sqrt{d}} W_k x_t + b_k, \quad (5)$$

$$v_t = W_v x_t + b_v, \quad (6)$$

$$i_t = \exp \left( w_i^\top x_t + b_i \right), \quad (7)$$

$$f_t = \exp \left( w_f^\top x_t + b_f \right), \quad (8)$$

$$o_t = \sigma \left( W_o x_t + b_o \right), \quad (9)$$

where the cell state  $C_t \in \mathbb{R}^{d \times d}$ ,  $n_t, h_t \in \mathbb{R}^d$  represent the normalizer state and the hidden state, respectively,  $\sigma(\cdot)$  is the sigmoid function, and  $\odot$  is element-wise multiplication. The input, forget and output gates are represented by  $i_t, f_t \in \mathbb{R}$  and  $o_t \in \mathbb{R}^d$ , respectively, while  $W_q, W_k, W_v \in \mathbb{R}^{d \times d}$  are learnable projection matrices and  $b_q, b_k, b_v \in \mathbb{R}^d$  are the respective biases for the query, key and value vectors. Finally,  $w_i, w_f \in \mathbb{R}^d$ , and  $W_o \in \mathbb{R}^{d \times d}$  represent the weights between the input  $x_t$  and the input, forget, and output gate, respectively, and  $b_i, b_f \in \mathbb{R}$  and  $b_o \in \mathbb{R}^d$  are their biases. Unlike LSTM and sLSTM, there are no interactions between hidden states from one time step to the following in mLSTM (i.e. no memory mixing). This means multiple memory cells and multiple heads are equivalent, allowing the forward pass to be parallelized.

## 2.2. xLSTM-SENet: speech enhancement with xLSTMs

For a direct comparison with the state-of-the-art dual-path [27] SE systems: SEMamba [21] and MP-SENet [14], we integrate xLSTM into the MP-SENet architecture by replacing the Conformer blocks with xLSTM blocks as shown in Figure 1. We use the MP-SENet architecture since it facilitates joint denoising of magnitude and phase spectra, and has shown superior performance compared to other time-frequency (TF) domain SE methods [14].

### 2.2.1. Model structure

**Model overview:** As shown in Figure 1, our proposed xLSTM-SENet architecture follows an encoder-decoder structure. Given the noisy speech waveform  $y \in \mathbb{R}^D$ , let  $Y = Y_m \cdot e^{jY_p} \in \mathbb{C}^{T \times F}$  (where  $T$  and  $F$  represent time and frequency dimensions, respectively) denote the corresponding complex spectrogram obtained through a short-time Fourier transform (STFT). We stack the wrapped phase spectrum  $Y_p \in \mathbb{R}^{T \times F}$  and the compressed magnitude spectrum  $(Y_m)^c \in \mathbb{R}^{T \times F}$  (extracted by applying power-law compression [28] with compression factor  $c = 0.3$  as in [14]) to create an input  $Y_{in} \in \mathbb{R}^{T \times F \times 2}$  to the feature encoder. The feature encoder encodes the input into a compressed TF-domain representation, which is subsequently fed to a stack of  $N$  TF-xLSTM blocks. Each TF-xLSTM block comprises a time and frequency xLSTM block, capturing temporal and frequency dependencies, respectively. Similar to SEMamba [21], we use a bidirectional architecture (Bi-mLSTM) for these blocks. Hence, the output  $v$  of the time and frequency xLSTM blocks is:

$$v = \text{Conv1d}(\text{mLSTM}(\varepsilon) \oplus \text{flip}(\text{mLSTM}(\text{flip}(\varepsilon))))), \quad (10)$$

where  $\varepsilon$  is the input to the time and frequency xLSTM blocks, and  $\text{mLSTM}(\cdot)$ ,  $\text{flip}(\cdot)$ ,  $\oplus$ , and  $\text{Conv1d}(\cdot)$  is the unidirectional mLSTM, the sequence flipping operation, concatenation, and the 1-D transposed convolution, respectively.

Finally, the output of the TF-xLSTM blocks is decoded by both a magnitude mask decoder and wrapped phase de-

coder [29]. They predict the clean compressed magnitude mask  $\mathbf{M}^c = (\mathbf{X}_m/\mathbf{Y}_m)^c \in \mathbb{R}^{T \times F}$  and the clean wrapped phase spectrum  $\mathbf{X}_p \in \mathbb{R}^{T \times F}$ , respectively. The enhanced magnitude spectrum  $\hat{\mathbf{X}}_m \in \mathbb{R}^{T \times F}$  is obtained by computing:

$$\hat{\mathbf{X}}_m = ((\mathbf{Y}_m)^c \odot \hat{\mathbf{M}}^c)^{1/c}, \quad (11)$$

where  $\hat{\mathbf{M}}^c$  is the predicted clean compressed magnitude mask. The final enhanced waveform  $\hat{\mathbf{x}}$  is reconstructed by performing an iSTFT on the enhanced magnitude spectrum  $\hat{\mathbf{X}}_m$  and the enhanced wrapped phase spectrum  $\hat{\mathbf{X}}_p$ .

Similar to MP-SENet [14] and SEMamba [21], we use a linear combination of loss functions which includes a PESQ-based GAN discriminator, along with time, magnitude, complex, and phase losses. We also employ the consistency loss function proposed in [30], as this has been shown to improve performance [21].

**Feature encoder:** Following MP-SENet [14], the encoder consists of two convolution blocks each comprising a 2D convolutional layer, an instance normalization, and parametric rectified linear unit (PReLU) activation, sandwiching a dilated DenseNet [31] with dilation sizes 1, 2, 4, and 8. The first convolutional block increases the input channels from 2 to  $C$ , while the second convolutional block halves the frequency dimension from  $F$  to  $F' = F/2$ , consequently reducing the computational complexity in the TF-xLSTM blocks. The dilated DenseNet extends the receptive field along the time axis, which facilitates long-range context aggregation over different resolutions.

**Magnitude mask and wrapped phase decoder:** Following MP-SENet [14], both the magnitude mask decoder and the wrapped phase decoder consist of a dilated DenseNet and a 2D transposed convolution. For the magnitude mask decoder, this is followed by a deconvolution block reducing the output channels from  $C$  to 1. To estimate the magnitude mask, we employ a learnable sigmoid function with  $\beta = 2$  as in [9]. In the wrapped phase decoder, the transposed convolution is followed by two parallel 2D convolutional layers outputting the pseudo-real and pseudo-imaginary part components. To predict the clean wrapped phase spectrum, we use the two-argument arctangent function (Arctan2) resulting in the enhanced wrapped phase spectrum  $\hat{\mathbf{X}}_p$ .

## 3. Experiments

### 3.1. Dataset

In this study, we perform experiments on the VoiceBank+Demand dataset, which consists of pairs of clean and noisy audio clips sampled at 48 kHz. The clean audio samples come from the VoiceBank corpus [15], which comprises 11,572 audio clips from 28 distinct speakers for training, and 824 audio clips from 2 distinct speakers for testing. The noisy audio clips are created by mixing the clean samples with noise from the DEMAND dataset [16] at four signal-to-noise ratios (SNRs) during training ([0, 5, 10, 15] dB) and testing ([2.5, 7.5, 12.5, 17.5] dB). Two speakers from the training set are left out as a validation set.

### 3.2. Implementation details

Unless otherwise stated, experimental details and training configurations match those presented in MP-SENet [14] and SEMamba [21]. To reduce memory and computational resources, all models were trained on randomly cropped 2-second audio clips. Additionally, all audio clips were downsampled to

16 kHz, reducing computational complexity and ensuring compatibility with the wide-band PESQ metric [32]. When performing STFTs we set the FFT order, Hann window size, and hop size to 400, 400, and 100, respectively. We train all models for 200 epochs and select the checkpoint (saved every 1000th step) with the best PESQ score on the validation data. We fix  $C = 64$  channels and  $N = 4$  stacks of TF-xLSTM blocks in our xLSTM-SENet model for direct comparison with SEMamba and MP-SENet. All models are trained with a batch-size  $B = 8$  on four NVIDIA L40S GPUs, and the four layer xLSTM-SENet model takes approximately 3 days to train. This is the main limitation of xLSTM compared to Mamba and Transformers, which are roughly four times as fast to train [23].

### 3.3. Evaluation metrics

We use the following commonly used evaluation metrics to assess SE performance: wide-band PESQ [32] and short-time objective intelligibility (STOI) [33]. To predict the signal distortion, background intrusiveness and overall speech quality, we use the composite measures CSIG, CBAK and COVL [34]. For all measures, a higher value is better. We train all models with 5 different seeds and document the mean and standard deviation.

## 4. Results and analysis

### 4.1. Comparison with existing methods

We evaluate several architectural design choices for our xLSTM-SENet model while limiting the parameter count to that of SEMamba. We choose the best model based on validation performance. Our best model uses a bidirectional architecture and we have added biases to layer normalizations and projection layers as in [25]. The expansion factor is set to  $E_f = 4$ .

Table 1: *Results on the VoiceBank+Demand dataset. “-” denotes that the result is not provided in the original paper. \* means the results are reproduced using the original provided code.*

Model	Params (M)	PESQ	CSIG	CBAK	COVL	STOI
Noisy	-	1.97	3.35	2.44	2.63	0.91
MetricGAN+ [9]	-	3.15	4.14	3.16	3.64	-
CMGAN [10]	1.83	3.41	4.63	3.94	4.12	0.96
DPT-FSNet [35]	0.88	3.33	4.58	3.72	4.00	0.96
Spiking-S4 [36]	0.53	3.39	4.92	2.64	4.31	-
TridentSE [37]	3.03	3.47	4.70	3.81	4.10	0.96
MP-SENet [14]	2.05	3.50	4.73	3.95	4.22	0.96
SEMamba [21]	2.25	3.55	4.77	3.95	4.26	0.96
MP-SENet*	2.05	3.49±0.02	4.72±0.02	3.92±0.04	4.22±0.02	0.96±0.00
SEMamba*	2.25	3.49±0.01	4.75±0.01	3.94±0.02	4.24±0.01	0.96±0.00
xLSTM-SENet	2.20	3.48±0.00	4.74±0.01	3.93±0.01	4.22±0.01	0.96±0.00

Table 1 shows that xLSTM-SENet matches the performance of the state-of-the-art SEMamba and MP-SENet models on the VoiceBank+Demand dataset, while outperforming other SE methods on most metrics. This demonstrates the effectiveness of xLSTM for SE.

### 4.2. Ablation study

To evaluate our model architecture design choices, we perform ablations on the expansion factor  $E_f$  and on the biases in layer normalizations and projection layers. Additionally, we investigate the performance of a unidirectional architecture, by remov-

ing the transposed convolution, flipping and the second mLSTM block within each time and frequency xLSTM block as shown in Figure 1. Since our xLSTM-SENet is bidirectional and thus has 2 mLSTM blocks, we double the amount of layers  $N$  for the unidirectional model. Finally, mLSTM adds exponential gating to improve LSTM, hence we evaluate its effect on speech enhancement performance by replacing it with sigmoid gating.

Table 2: Ablation study on the VoiceBank+Demand dataset. Default settings for xLSTM-SENet:  $E_f = 4$ , a bidirectional architecture, and biases in layer normalizations and projection layers.

Model	Params (M)	PESQ	CSIG	CBAK	COVL	STOI
Noisy	-	1.97	3.35	2.44	2.63	0.91
xLSTM-SENet	2.20	3.48±0.00	4.74±0.01	3.93±0.01	4.22±0.01	0.96±0.00
$E_f = 3$	1.96	3.46±0.01	4.72±0.00	3.93±0.02	4.21±0.01	0.96±0.00
$E_f = 2$	1.71	3.45±0.01	4.71±0.01	3.92±0.01	4.19±0.01	0.96±0.00
w/o Biases	2.18	3.46±0.00	4.72±0.01	3.91±0.01	4.20±0.02	0.96±0.00
Unidirectional	2.14	3.26±0.02	4.57±0.02	3.79±0.01	4.00±0.02	0.95±0.00
w/o Exp. gating	2.20	3.45±0.02	4.72±0.02	3.90±0.01	4.20±0.03	0.96±0.00

Table 2 shows that decreasing the expansion factor  $E_f$  decreases performance. Moreover, as in Vision-LSTM [25], biases in layer normalizations and projection layers improve performance. We also find that a bidirectional architecture significantly outperforms a unidirectional architecture. Finally, we find that exponential gating improves performance for SE, which was not the case for learning self-supervised audio representations with xLSTMs [26].

### 4.3. Comparison with LSTM

To compare the performance of xLSTM and LSTM for SE, we first replace the mLSTM layers in xLSTM-SENet with conventional LSTM layers (this model is referred to as: LSTM (layer)). Table 3 shows that this results in a performance decrease even though LSTM (layer) is approximately 11% larger. Then, we replace the entire mLSTM block with LSTM (denoted as: LSTM (block)) and double the number of layers  $N$  to roughly match the parameter count of xLSTM-SENet. Table 3 shows that LSTM (block) matches xLSTM-SENet in performance, which in Table 1 was shown to match the performance of state-of-the-art Mamba and Conformer-based systems.

Table 3: Comparison of xLSTM with LSTM on the VoiceBank+Demand dataset.

Model	Params (M)	PESQ	CSIG	CBAK	COVL	STOI
Noisy	-	1.97	3.35	2.44	2.63	0.91
xLSTM-SENet	2.20	3.48±0.00	4.74±0.01	3.93±0.01	4.22±0.01	0.96±0.00
LSTM (layer)	2.44	3.44±0.01	4.69±0.02	3.90±0.00	4.17±0.01	0.96±0.00
LSTM (block)	2.34	3.49±0.02	4.76±0.01	3.95±0.01	4.24±0.01	0.96±0.00

### 4.4. Scaling experiments

Smaller models are preferred in real-world SE applications, like hearing aids, due to reduced computational complexity, facilitating their use in such devices. Additionally, it is of interest to explore the performance achieved by increasing model sizes. Hence, we perform a comparative analysis of xLSTM, Mamba, Conformer and LSTM across varying layer counts  $N$ .

For LSTM,  $N$  is doubled to roughly match the parameter counts of the xLSTM-, Mamba-, and Conformer-based models.

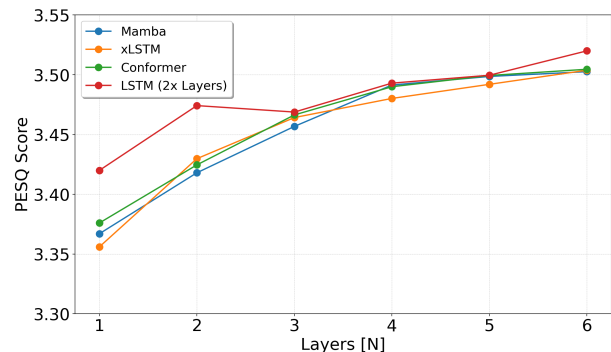


Figure 2: Scaling results on the VoiceBank+Demand dataset. The smallest ( $N = 1$ ) and largest ( $N = 6$ ) models are 1.37 M and 2.94 M parameters, respectively.

Figure 2 shows that xLSTM, Mamba, and Conformer-based models perform similarly when scaled down, with LSTM outperforming them for  $N = 1$  and  $N = 2$ . When scaled up, all models achieve comparable performance. For  $N = 1$ , training-time is reduced by nearly 70% compared to  $N = 4$ .

### 4.5. xLSTM-SENet2

To investigate the benefits of increased depth over width in xLSTM for SE, we propose xLSTM-SENet2, which is configured with an expansion factor  $E_f = 2$  and  $N = 8$  layers. This allows for a deeper architecture while maintaining a comparable parameter count to xLSTM-SENet. Table 4 shows that xLSTM-SENet2 outperforms state-of-the-art LSTM-, Mamba-, and Conformer-based models.

Table 4: Speech enhancement performance of xLSTM-SENet2 on the VoiceBank+Demand dataset. \* means the results are reproduced using the original provided code.

Model	Params (M)	PESQ	CSIG	CBAK	COVL	STOI
Noisy	-	1.97	3.35	2.44	2.63	0.91
LSTM (block)	2.34	3.49±0.02	4.76±0.01	3.95±0.01	4.24±0.01	0.96±0.00
MP-SENet*	2.05	3.49±0.02	4.72±0.02	3.92±0.04	4.22±0.02	0.96±0.00
SEMamba*	2.25	3.49±0.01	4.75±0.01	3.94±0.02	4.24±0.01	0.96±0.00
xLSTM-SENet2	2.27	3.53±0.01	4.78±0.01	3.98±0.02	4.27±0.01	0.96±0.00

## 5. Conclusion

This paper proposed xLSTM-SENet, an Extended Long Short-Term Memory-based model for speech enhancement. Experiments on the VoiceBank+Demand dataset show that xLSTM-SENet, and even LSTM-based models, rival existing state-of-the-art Mamba- and Conformer-based speech enhancement systems across several model sizes. We studied the importance of several architectural design choices, and demonstrated that the inclusion of exponential gating and bidirectionality is critical to the performance of the xLSTM-SENet model. Finally, empirical results show that our best xLSTM-based system, xLSTM-SENet2, outperforms state-of-the-art speech enhancement systems on the VoiceBank+Demand dataset.

## 6. References

- [1] M. Kolbæk, Z.-H. Tan, and J. Jensen, “Speech intelligibility potential of general and specialized deep neural network based speech enhancement systems,” *IEEE/ACM Transactions on Audio, Speech, and Language Processing*, vol. 25, no. 1, pp. 153–167, 2016.
- [2] Z. Chen, S. Watanabe, H. Erdogan, and J. R. Hershey, “Speech enhancement and recognition using multi-task learning of long short-term memory recurrent neural networks,” in *INTER-SPEECH*, 2015, pp. 3274–3278.
- [3] S. Shon, H. Tang, and J. Glass, “Voiceid loss: Speech enhancement for speaker verification,” in *INTER-SPEECH*, 2019, pp. 2888–2892.
- [4] K. Tesch, N.-H. Mohrmann, and T. Gerkmann, “On the role of spatial, spectral, and temporal processing for dnn-based non-linear multi-channel speech enhancement,” in *INTER-SPEECH*, 2022, pp. 2908–2912.
- [5] S.-W. Fu, Y. Tsao, X. Lu *et al.*, “Snr-aware convolutional neural network modeling for speech enhancement,” in *INTER-SPEECH*, 2016, pp. 3768–3772.
- [6] M. Kolbæk, Z.-H. Tan, S. H. Jensen, and J. Jensen, “On loss functions for supervised monaural time-domain speech enhancement,” *IEEE/ACM Transactions on Audio, Speech, and Language Processing*, vol. 28, pp. 825–838, 2020.
- [7] D. Michelsanti and Z.-H. Tan, “Conditional generative adversarial networks for speech enhancement and noise-robust speaker verification,” in *INTER-SPEECH*, 2017, pp. 2008–2012.
- [8] S.-W. Fu, C.-F. Liao, Y. Tsao, and S.-D. Lin, “Metricgan: Generative adversarial networks based black-box metric scores optimization for speech enhancement,” in *International Conference on Machine Learning (ICML)*, 2019, pp. 2031–2041.
- [9] S.-W. Fu, C. Yu, T.-A. Hsieh, P. Plantinga, M. Ravanelli, X. Lu, and Y. Tsao, “Metricgan+: An improved version of metricgan for speech enhancement,” in *INTER-SPEECH*, 2021, pp. 201–205.
- [10] S. Abdulatif, R. Cao, and B. Yang, “Cmgan: Conformer-based metric-gan for monaural speech enhancement,” *IEEE/ACM Transactions on Audio, Speech, and Language Processing*, 2024.
- [11] Y.-J. Lu, Z.-Q. Wang, S. Watanabe, A. Richard, C. Yu, and Y. Tsao, “Conditional diffusion probabilistic model for speech enhancement,” in *IEEE ICASSP*, 2022, pp. 7402–7406.
- [12] J. Richter, S. Welker, J.-M. Lemerrier, B. Lay, and T. Gerkmann, “Speech enhancement and dereverberation with diffusion-based generative models,” *IEEE/ACM Transactions on Audio, Speech, and Language Processing*, vol. 31, pp. 2351–2364, 2023.
- [13] P. Gonzalez, Z.-H. Tan, J. Østergaard, J. Jensen, T. S. Alstrøm, and T. May, “Investigating the design space of diffusion models for speech enhancement,” *IEEE/ACM Transactions on Audio, Speech, and Language Processing*, 2024.
- [14] Y.-X. Lu, Y. Ai, and Z.-H. Ling, “Mp-senet: A speech enhancement model with parallel denoising of magnitude and phase spectra,” in *INTER-SPEECH*, 2023, pp. 3834–3838.
- [15] C. Veaux, J. Yamagishi, and S. King, “The voice bank corpus: Design, collection and data analysis of a large regional accent speech database,” in *IEEE International Conference Oriental COCOSDA held jointly with 2013 Conference on Asian Spoken Language Research and Evaluation (O-COCOSDA/CASLRE)*, 2013, pp. 1–4.
- [16] J. Thiemann, N. Ito, and E. Vincent, “The diverse environments multi-channel acoustic noise database (demand): A database of multichannel environmental noise recordings,” in *Proceedings of Meetings on Acoustics*, vol. 19, no. 1. AIP Publishing, 2013.
- [17] D. de Oliveira, T. Peer, and T. Gerkmann, “Efficient transformer-based speech enhancement using long frames and stft magnitudes,” in *INTER-SPEECH*, 2022, pp. 2948–2952.
- [18] Y. Gong, Y.-A. Chung, and J. Glass, “Ast: Audio spectrogram transformer,” in *INTER-SPEECH*, 2021, pp. 571–575.
- [19] A. Gu and T. Dao, “Mamba: Linear-time sequence modeling with selective state spaces,” in *First Conference on Language Modeling (COLM)*, 2024.
- [20] S. Yadav and Z.-H. Tan, “Audio mamba: Selective state spaces for self-supervised audio representations,” in *INTER-SPEECH*, 2024, pp. 552–556.
- [21] R. Chao, W.-H. Cheng, M. La Quatra, S. M. Siniscalchi, C.-H. H. Yang, S.-W. Fu, and Y. Tsao, “An investigation of incorporating mamba for speech enhancement,” in *IEEE Spoken Language Technology Workshop*, 2024.
- [22] J. Schmidhuber, S. Hochreiter *et al.*, “Long short-term memory,” *Neural Computation*, vol. 9, no. 8, pp. 1735–1780, 1997.
- [23] M. Beck, K. Pöppel, M. Spanring, A. Auer, O. Prudnikova, M. K. Kopp, G. Klambauer, J. Brandstetter, and S. Hochreiter, “xLSTM: Extended long short-term memory,” in *The Thirty-eighth Annual Conference on Neural Information Processing Systems (NeurIPS)*, 2024.
- [24] K. Tesch and T. Gerkmann, “Multi-channel speech separation using spatially selective deep non-linear filters,” *IEEE/ACM Transactions on Audio, Speech, and Language Processing*, vol. 32, pp. 542–553, 2023.
- [25] B. Alkin, M. Beck, K. Pöppel, S. Hochreiter, and J. Brandstetter, “Vision-1stm: xlstm as generic vision backbone,” in *The Thirteenth International Conference on Learning Representations (ICLR)*, 2025.
- [26] S. Yadav, S. Theodoridis, and Z.-H. Tan, “Audio xlstms: Learning self-supervised audio representations with xlstms,” in *INTER-SPEECH (Accepted)*, 2025.
- [27] Y. Luo, Z. Chen, and T. Yoshioka, “Dual-path rnn: efficient long sequence modeling for time-domain single-channel speech separation,” in *IEEE ICASSP*, 2020, pp. 46–50.
- [28] S. Wisdom, J. R. Hershey, K. Wilson, J. Thorpe, M. Chinen, B. Patton, and R. A. Saurous, “Differentiable consistency constraints for improved deep speech enhancement,” in *IEEE ICASSP*, 2019, pp. 900–904.
- [29] Y. Ai and Z.-H. Ling, “Neural speech phase prediction based on parallel estimation architecture and anti-wrapping losses,” in *IEEE ICASSP*, 2023, pp. 1–5.
- [30] V. Zadorozhnyy, Q. Ye, and K. Koishida, “Scp-gan: Self-correcting discriminator optimization for training consistency preserving metric gan on speech enhancement tasks,” in *INTER-SPEECH*, 2023, pp. 2463–2467.
- [31] A. Pandey and D. Wang, “Densely connected neural network with dilated convolutions for real-time speech enhancement in the time domain,” in *IEEE ICASSP*, 2020, pp. 6629–6633.
- [32] A. W. Rix, J. G. Beerends, M. P. Hollier, and A. P. Hekstra, “Perceptual evaluation of speech quality (pesq)-a new method for speech quality assessment of telephone networks and codecs,” in *IEEE ICASSP*, vol. 2, 2001, pp. 749–752.
- [33] C. H. Taal, R. C. Hendriks, R. Heusdens, and J. Jensen, “An algorithm for intelligibility prediction of time–frequency weighted noisy speech,” *IEEE Transactions on audio, speech, and language processing*, vol. 19, no. 7, pp. 2125–2136, 2011.
- [34] Y. Hu and P. C. Loizou, “Evaluation of objective quality measures for speech enhancement,” *IEEE Transactions on audio, speech, and language processing*, vol. 16, no. 1, pp. 229–238, 2007.
- [35] F. Dang, H. Chen, and P. Zhang, “Dpt-fsnet: Dual-path transformer based full-band and sub-band fusion network for speech enhancement,” in *IEEE ICASSP*, 2022, pp. 6857–6861.
- [36] Y. Du, X. Liu, and Y. Chua, “Spiking structured state space model for monaural speech enhancement,” in *IEEE ICASSP*, 2024, pp. 766–770.
- [37] D. Yin, Z. Zhao, C. Tang, Z. Xiong, and C. Luo, “Tridentse: Guiding speech enhancement with 32 global tokens,” in *INTER-SPEECH*, 2023, pp. 3839–3843.